agronomy

MDPI

Article

Aboveground Structural Attributes and Morpho-Anatomical Response Strategies of *Bromus valdivianus* Phil. and *Lolium perenne* L. to Severe Soil Water Restriction

Yongmei Zhang [1], Javier García-Favre [2], Haiying Hu [3], Ignacio F. López [4,*], Iván P. Ordóñez [5], Andrew D. Cartmill [4] and Peter D. Kemp [4]

1 State Key Lab of Aridland Crop Science, Gansu Agricultural University, Lanzhou 730070, China; zhangyongm@gsau.edu.cn
2 Facultad de Agronomía, Universidad de la República, Montevideo 12900, Uruguay; jgfavre@fagro.edu.uy
3 Science &Technology Department, Ningxia University, Yinchuan 750021, China; haiying@nxu.edu.cn
4 School of Agriculture and Environment, Massey University, Palmerston North 4442, New Zealand; a.cartmill@massey.ac.nz (A.D.C.); p.kemp@massey.ac.nz (P.D.K.)
5 Instituto de Investigaciones Agropecuarias, INIA Kampenaike, Punta Arenas 6200000, Chile; ivan.ordonez@inia.cl
* Correspondence: i.f.lopez@massey.ac.nz

Abstract: Grass species have a range of strategies to tolerate soil water restriction, which are linked to the environmental conditions at their site of origin. Climate change enhances the relevance of the functional role of anatomical attributes and their contribution as water stress tolerance factors. Morpho-anatomical traits and adjustments that contribute to drought resistance in *Lolium perenne* L. (Lp) and *Bromus valdivianus* Phil. (Bv), a temperate humid grass species, were analysed. The structure of the leaves and pseudostems (stems only in Lp) grown at 20–25% field capacity (FC) (water restriction) and 80–85% FC (control) were evaluated by making paraffin sections. In both species, water restriction reduced the thickness of the leaves and pseudostems, along with the size of the vasculature. Bv had long and dense leaf hairs, small and numerous stomata, and other significant adaptive traits under water stress, including thicker pseudostems ($p \leq 0.001$), a greatly thickened bundle sheath wall ($p \leq 0.001$) in the pseudostem to ensure water flow, and a thickened cuticle covering on leaf surfaces ($p \leq 0.01$) to avoid water loss. Lp vascular bundles developed throughout the stem, and under water restriction the xylem vessel walls were strengthened and lignified. Lp leaves had individual traits of a ribbed/corrugated-shaped upper surface, and the stomata were positioned to maintain relative humidity outside the leaf surface. Water restriction significantly changed the bulliform cell depth in Lp ($p \leq 0.05$) that contributed to water loss reduction via the curling leaf blade. This study demonstrated that the two grass species, through different morphological traits, were able to adjust their individual tissues and cells in aboveground parts to reach similar physiological functions to reduce water loss with increased water restriction. These attributes explain how both species enhance persistence and resilience under soil water restriction.

Keywords: tolerance; growth strategies; stomata; photosynthesis; water conductance; field capacity; permanent wilting point

Citation: Zhang, Y.; García-Favre, J.; Hu, H.; López, I.F.; Ordóñez, I.P.; Cartmill, A.D.; Kemp, P.D. Aboveground Structural Attributes and Morpho-Anatomical Response Strategies of *Bromus valdivianus* Phil. and *Lolium perenne* L. to Severe Soil Water Restriction. *Agronomy* **2023**, *13*, 2964. https://doi.org/10.3390/agronomy13122964

Academic Editor: Tomasz Głąb

Received: 24 October 2023
Revised: 22 November 2023
Accepted: 27 November 2023
Published: 30 November 2023

1. Introduction

Climate change and the increasing concentrations of greenhouse gases are projected to elevate global surface temperatures, potentially magnify the intensity and variability of seasonal precipitation and drought events [1], and threaten the long-term resilience and sustainability of agroecosystems [2]. Pasture-based production systems are geographically extensive and may be especially sensitive to drought events [3].

Pasture responses to water stress (drought events) are complex, multifaceted, and not fully understood. Under drought conditions, pasture productivity, persistence, and livestock performance are dependent on a variety of factors, including the climate, grass species (species mixture), stocking rates, pasture management, and production goals. This is further impacted by the interplay in soil water availability, grass species morpho-physiology, and species-dependent drought resistance strategies. For example, large differences in leaf water potential and cavitation resistance (hydraulic failure) have been observed in a variety of grass species under drought conditions [4,5]; for example, *Agrostis capillaris* L., *Anthoxanthum odoratum* L., and *Festuca arundinacea* Schreb were reported to be highly drought tolerant, while *Poa pratensis* L. was classified as being less drought tolerant. Cultivars of *Lolium perenne* L. and *Dactylis glomerata* L. were suggested to be within the drought tolerance range as a result of the environment to which these species are found [4].

Stomatal conductance and lamina osmotic adjustment, coupled with a deep root system (which exploits deeper wetter portions of the soil profile), enhances *F. arundinacea* drought adaptability and survival. However, cultivars of *F. arundinacea* have been reported to vary in stomatal conductance and lamina osmotic adjustment according to their climatic origins (mediterranean vs. temperate) [6]. Similar climatic constraints were also reported for *D. glomerata* [7] in that distinct differences in the thickness of the metaxylem vessel wall and embolism tolerance were observed in the stem, with decreased summer precipitation depending on the climatic origin of the plant material. The mediterranean population had thicker metaxylem vessel walls and greater embolism tolerance when compared to the northern and temperate populations, with the temperate population having the thinnest metaxylem vessel walls and lowest embolism tolerance [7]. In addition, the thickness of the cell wall and cuticle, as described for the *Zea mays* L. lines, is another morpho-anatomical feature that reduces water loss [8] in that thicker epidermal cell walls and cuticles lowered the rates of water loss. Drought tolerance of *Panicum coloratum* L. (kleingrass) increased with the development of sclerenchyma tissue and increased thickness of the leaf metaxylem cell walls [9].

Thus, grass species exhibit several morpho-anatomical responses to reduced soil water availability, which demonstrate fitness to the specific environmental constraints associated with drought [10,11]. However, differences in species fitness to dry conditions (i.e., summer droughts) may result in species segregation, with the selection of ecotypes (individual plants or group of plants) to distinct climatic conditions or sites [12]. Ecotypes of grass species may further modify morpho-anatomical structures in response to water stress. Phenotypic plasticity also contributes to enhance plant species drought tolerance, survival, and ecosystem population stability [10,13–15].

Lolium perenne (Lp: perennial ryegrass) is a fast-growing, high-yielding perennial grass, with good palatability and quality [16]. It is native to Central Asia, the Middle East, North Africa, and Southern Europe, and is widely cultivated and naturalised around the world. *Bromus valdivianus* Phil. (Bv: pasture brome), is a fast-growing, drought-tolerant perennial grass, native to temperate humid regions of South America [17,18], with an annual yield and herbage quality similar to Lp [19] (Calvache et al. 2020), but with a greater leaf area, tiller weight, and lower tiller density when compared to Lp [17,20]. In the south of Chile, Lp and Bv co-dominate, creating highly productive naturalised pastures [21] with complex webs of both intra- and inter-specific interactions. For example, when both species were subjected to soil water restriction (20–25% field capacity; FC), similar aboveground mass was produced by each species through different growth strategies in that the physiological regulation of tiller development highlights a trade-off between lamina growth and root mass per tiller in relation to the tiller population [17,18]. However, very little additional information is available about the adaptive morphological and anatomical traits, and the modifications of Lp and Bv in relation to water movement, when these species are grown under limiting soil water conditions.

Plant responses to water restriction stress are linked to the physiological properties of cellular components and to the morpho-anatomical characteristics of tissues that regulate

water transmission and/or movement [22,23]. Phenotypic plasticity may also constitute a plant survival strategy in response to water restriction stress related to anatomical mechanisms [23,24]. Bv and Lp have contrasting growth strategies. Bv is a six-leaf species [20,25] that favours leaf number, total leaf length per tiller, and also leaf and tiller size over tiller density; meanwhile, Lp presents a contrasting scenario [17,25,26], being a three-leaf species [27,28] that compensates for its lower tiller mass with a higher tiller population density [17,29].

Therefore, the objectives of this study were to: (i) examine and analyse the morpho-anatomical traits of the Bv and Lp leaf blades and pseudostems (or stems) when grown under soil water-limiting conditions, and (ii) investigate the role of these structural adjustments for the maintenance of plant water flow and reduction in plant water loss. We hypothesised that temperate humid grass species of different origins possess distinct individual structural attributes and anatomical adaptations that promote survival under long-term drought conditions.

2. Materials and Methods

2.1. Preparation

This study was carried out under glasshouse conditions at the Plant Growth Unit (40.37° latitude south and 175.61° longitude west), School of Agriculture and Environment, Massey University, Palmerston North, New Zealand, from September 2018 to March 2019. The average temperatures consisted of a minimum of 19.3 °C, a maximum of 27.1 °C, a daily average of 22.2 °C, and 60.2% relative humidity. The average PAR was 84.1 µmol m^{-1} s^{-1}.

Pots (20 × 20 cm) were filled with 3.8 kg of dry substrate. The planting substrate was composed of 30% Manawatu silt loam soil and 70% fine sand (by volume), which was modified with 60 g of long-term fertiliser, 30 g of short-term fertiliser, and 45 g of dolomite per 60 kg of substrate. The substrate chemical status was: pH 6.3 (soil: water = 1:2), 35 Olsen-P mg L^{-1}, 0.34 exchangeable K me 100 g^{-1}, 2.4 exchangeable Ca me 100 g^{-1}, 0.60 exchangeable Mg me 100 g^{-1}, <0.05 exchangeable Na me 100 g^{-1}, 3.0 CEC me 100 g^{-1}, and 83 SO_4^{2-} mg kg^{-1}.

Half the pots were sown (23 September 2018) with two seeds of *Bromus valdivianus* Phil. cv. Bareno, and the remaining pots were sown with two *Lolium perenne* L. cv. Trojan seeds (Barenbrug, ChCh, Christchurch, New Zealand). The pots were irrigated, and the substrate was maintained at FC. Following seedling emergence, the pots were thinned to one plant (3 October 2018), and the plants were grown at 80–85% FC (volumetric soil water content (VWC)) for 12 weeks prior to establishing the soil water restriction treatments.

2.2. Water Restriction Treatments

The substrate water retention curve was determined using 100 cm^3 metallic cylinders (n = 3). Field capacity was reached at 16% of VWC and permanent wilting point (PWP) at 2% VWC. The substrate water restriction treatments used in the study were 80–85% FC (FC–80–85% (FC–PWP)) and 20–25% FC (FC–20–25% (FC–PWP)) (severe water restriction treatment (water restriction)), equivalent to 13.2–14% and 4.8–5.5% VWC, respectively, alongside a no water restriction treatment (control).

The study was laid out as a randomised complete block design (5 blocks), with factorial treatment distribution [30], two species (Lp and Bv), and two levels of soil water restriction (control and water restriction). The water restriction period went from 23 December 2018 to 17 January 2019. The substrate water content was measured daily (Mini Trace with soil-moisture TDR Technology, Soilmoisture Equipment Corp., Goleta, CA, USA) and adjusted as needed.

Five additional blocks of Lp and Bv under the same two water restriction levels were grown adjacent to the experimental pots and used for daily TDR measurements, thereby avoiding soil and root disturbances in the experimental units. Thus, the TDR data collected from each Bv and Lp treatment were utilised, as described by the authors of [17,31], to calculate the daily water loss from each treatment and the irrigation volume

of water reposition to each individual pot according to the water restriction treatment. The volume of water added daily was calculated using the following formula:

$$I = \frac{(IC - WC)}{100} \times SW \quad (1)$$

where I: irrigation (kg); IC: irrigation criteria (% in volume); WC: substrate soil water content (% in volume); and SW: substrate soil's dry weight (kg).

2.3. Plant Measurement

Plant tiller number (block, $n = 5$) was recorded at 7 days, 13 days, 19 days, and 25 days after application of the water treatments. At day 26 (17 January 2019), photosynthetic indices were measured (LI-COR 6400 Portable Photosynthesis System; LI-COR Biosciences, Lincoln, NE, USA), between 9:00–11:00 a.m. on the second fully expanded leaf of an individual tiller, measuring a total of 3 tillers per pot, treated as 3 subsamples per pot per block. Individual tiller water potential ($\Psi w = -P$) was then measured ($n = 5$) (Scholander Pressure Chamber; Soilmoisture Equipment Corp., Goleta, CA, USA) between 11:00 a.m.–12:00 p.m. on the second fully expanded leaf from one tiller per pot. The newest fully expanded leaf of an individual tiller per pot was collected ($n = 5$) and stored (−20 °C) for determination of osmotic potential (HR-33T Dew Point Microvoltmeter, Wescor, Logan, UT, USA).

Features of foliage anatomy were also measured from 3 tillers per pot (3 subsamples per pot per block; block, $n = 5$), with each pot acting as an experimental unit. Intact tillers of similar ages (leaf stage) and development as those used for the photosynthesis, water potential, and osmotic potential measurements were collected. Care was taken to ensure that the lamina and sheath sampled were of a second fully expanded leaf. Samples of 1 cm long were taken from the leaf blade and pseudostem or stem. The leaf blade sample corresponded to a cutting from the middle of the second fully expanded leaf blade (half of the distance between the ligule and the lamina tip). The pseudostem (and/or stem) was accurately sampled from 1 cm above the junction of the root and the stem (root neck). All samples were fixed in F.A.A. solution (formalin–acetic acid–alcohol solution: 70% ethanol: glacial acetic acid: formaldehyde in a 90:5:5 ratio by volume) immediately after collection [32].

The remaining plant material from each pot was harvested and separated into shoots and roots; the roots were washed, and the plant material was oven dried at 70 °C for 72 h or until they reached a constant dry mass (DM).

2.4. Observation of Leaf Surface

Leaf surfaces, including leaf hairs (trichomes) and stomata, were observed on 12-week-old Lp and Bv grown in the 5 supernumerary pots before the commencement of the water restriction treatments. Adaxial or abaxial leaf sections 1 cm long from the middle of the second fully expanded leaf blade were cut, and the leaf hairs and stomata in Bv and the leaf hairs in Lp were observed, following the same method described previously, with 3 tillers subsampled per pot per block (block, $n = 5$) (Leica MZ12 stereomicroscope, Bourne End, Buckinghamshire, UK). This procedure was modified for the thicker Lp leaves in that the lower epidermis layer was peeled off and then observed for stomata.

2.5. Paraffin Sections

Following fixation in F.A.A. solution for 24 h, leaf blade and pseudostem samples were removed and rinsed twice with 50% isopropanol for 45 min. The samples were then processed, as described by the authors of [33]. Briefly, sample dehydration was achieved in 70%, 85%, and 95% isopropanol (including 1% eosin) at room temperature for 45 min. To reach absolute dehydration, the samples were dipped for 30 min in 100% isopropanol three times. Transparency of samples was obtained through a decreasing gradient of isopropanol and increasing levels of mineral oil for 30 min at 60 °C or until 100% of the mineral oil had fully entered the sample. The mineral oil within the samples was then

replaced with paraplast X-tra. Paraplast X-tra replacement was repeated 5 times every 2.5–3 h at 60 °C. The samples were then stored in paraplast X-tra prior to embedding.

Leaf and pseudostem samples of the same treatment were embedded (Leica HistoCore Arcadia with Arcadia H and Arcadia C, Leica Biosystems, Mt. Waverely, VIC, Australia) in long thin paper boats filled with 62 °C paraffin. Solidified paraffin blocks were then trimmed and pasted into microtome cartridges using hot paraffin. A series of transversal sections were obtained using a rotary microtome (Leica RM2265, Leica Biosystems, Mt. Waverely, VIC, Australia). The sections were 8 µm, 10 µm, or 15 µm in thickness and were collected on microscope slides. The slides were then dried at 40 °C for ~72 h, stained in safranin for 9 h, and re-dyed in fast green for 20 s. The sections were observed under a microscope (Olympus BX51, Mt. Waverley, VIC, Australia), and images were captured via CCD (Olympus SC30, Mt. Waverley, VIC, Australia). The size of the structures in the images was then measured (cellSens 2.1 Software, Olympus, Mt. Waverley, VIC, Australia).

2.6. Statistical Analysis

The data were analysed for normal distribution and homogeneity of variance. Kolmogorov–Smirnov and Bartlett's tests were applied prior to ANOVA with the GLM procedure. The differences among treatments means were explored using the LSD test. Canonical variate analysis (CVA) was also performed. Variables were standardised with the following equation:

$$Z = (yi - \bar{y})/St.\ Dev. \quad (2)$$

where Z: standardised variable; y: original variable; $\bar{y}$: mean; and St. Dev.: standard deviation [34]. All statistical analyses were performed using SAS (Statistical Analysis System) software version 9.2 (SAS Institute, Inc., Cary, NC, USA).

3. Results

3.1. Herbage and Root Biomass, Water Status, and Photosynthesis

Lolium perenne had a significantly higher ($p \leq 0.001$) tiller number (×2.5) per plant when compared to Bv under both soil water conditions, which explained the significant ($p \leq 0.001$) interaction observed between species and water restriction levels in that Bv tiller number plant^{-1} dropped by 50.4% due to the water restriction from 48.0 tillers plant^{-1} in the control to 23.8 tillers plant^{-1}, and Lp tiller number plant^{-1} decreased by 50.8% from 122.8 tillers plant^{-1} to 60.4 tillers plant^{-1} ($p \leq 0.001$; Table 1; Figure 1).

Table 1. Tiller number, accumulated aerial dry mass, root dry mass, and root-to-aerial biomass ratio for *Bromus valdivianus* (Bv) and *Lolium perenne* (Lp) grown at 80–85% FC and 20–25% FC (mean ± sem; $n = 5$).

	Tiller Number per Plant	Aerial DM (g/Plant)	Root DM (g/Plant)	Root–Shoot Ratio
Species				
Bv	35.90 ± 4.12	8.51 ± 1.58	2.56 ± 0.42	0.38 ± 0.03
Lp	91.60 ± 10.66	7.90 ± 1.65	2.40 ± 0.55	0.31 ± 0.02
Significance	***	ns	ns	ns
Soil water content				
80–85% FC	85.40 ± 12.67	12.97 ± 0.92	3.58 ± 0.45	0.28 ± 0.02
20–25% FC	42.10 ± 6.20	3.44 ± 0.18	1.37 ± 0.10	0.41 ± 0.03
Significance	***	***	***	***
Species × soil water content				
Bv × 80–85% FC	48.00 ± 1.05 c	13.87 ± 0.50	3.65 ± 0.42	0.29 ± 0.03 b
Bv × 20–25% FC	23.80 ± 1.50 d	3.16 ± 0.26	1.47 ± 0.10	0.47 ± 0.02 a
Lp × 80–85% FC	122.80 ± 4.66 a	12.08 ± 1.87	3.51 ± 0.85	0.28 ± 0.03 b
Lp × 20–25% FC	60.40 ± 1.83 b	3.72 ± 0.19	1.28 ± 0.16	0.34 ± 0.03 b
Significance	***	ns	ns	*

ANOVA and LSD test; * $p \leq 0.05$; ** $p \leq 0.01$; *** $p \leq 0.001$; ns, not significant ($p > 0.05$); and FC, field capacity.

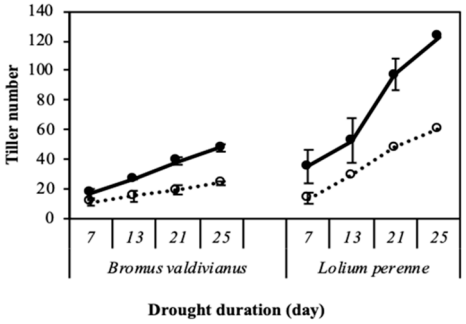

Figure 1. Tiller numbers of *Bromus valdivianus* and *Lolium perenne* exposed to water treatments at 80~85% FC (●) and 20~25% FC (○) (means ± sem; n = 5).

There were no significant differences between Bv and Lp in aerial and root DM or interactions between the main effects. However, water restriction significantly ($p \leq 0.001$) reduced aerial and root biomass for both species by 73.5% and 61.7%, respectively (Table 1), resulting in a significant ($p \leq 0.05$) interaction between species and water restriction, when the root–shoot ratio was analysed. In general, the root–shoot ratio under water restriction increased for both species. The Bv root–shoot ratio significantly increased from 0.29 to 0.47 (62%), while the Lp root–shoot ratio increased (21.4%) in general but was not significant under water restriction when compared to the control.

Both grass species had similar water potential (WP), osmotic potential (OP), photosynthetic rate (Photo), water conductance (Cond), intercellular CO_2 concentration (Ci), transpiration rate (Trmmol), temperature difference between leaf thermocouple and sample cell (Tl-Ta), water content difference between intercellular water and sample cellular water (H_2Odiff), and surface humidity values (RHsfc) ($p > 0.05$; Table 2). The Photo, Trmmol, and Tl-Ta of both species did not significantly vary due to the soil water restriction. However, Photo and Ci diminished by 11% and 21%, respectively, suggesting a restriction of the photosynthetic ability in both species. Furthermore, Cond was reduced by 43% ($p \leq 0.05$), and the WP and OP increased ($p \leq 0.001$) in the leaves by 42% and 26%, respectively (Table 2).

Table 2. Photosynthesis and water status in *Bromus valdivianus* (Bv) and *Lolium perenne* (Lp) grown at 80–85% FC and 20–25% FC. (mean ± sem; n = 5).

	Water Potential (Mpa)	Osmotic Potential (Mpa)	Photo (μmCO_2/ m^2s)	Cond ($molH_2O$/ m^2s)	Ci ($\mu molCO_2$/ m^2s)	Trmmol ($mmolH_2O$/ m^2s)	Tl-Ta (°C)	H_2Odiff ($mmolH_2O$/ mol)	RHsfc (%)
Species									
Bv	−1.86 ± 0.12	−2.05 ± 0.13	12.36 ± 1.22	0.18 ± 0.03	239.3 ± 10.50	3.72 ± 0.46	−0.05 ± 0.24	22.87 ± 0.99	44.61 ± 2.19
Lp	−1.76 ± 0.11	−1.88 ± 0.11	9.94 ± 0.39	0.15 ± 0.02	247.2 ± 13.35	3.21 ± 0.26	0.21 ± 0.14	23.22 ± 0.85	42.84 ± 1.45
Significance	ns	ns	ns	ns	ns	ns	ns	ns	ns
Soil water content									
80–85% FC	−1.33 ± 0.12	−1.67 ± 0.07	11.81 ± 1.13	0.21 ± 0.03	271.6 ± 6.78	4.02 ± 0.38	−0.21 ± 0.20	20.68 ± 0.52	47.55 ± 1.62
20–25% FC	−2.29 ± 0.11	−2.26 ± 0.06	10.49 ± 0.83	0.12 ± 0.01	214.9 ± 8.07	2.91 ± 0.28	0.37 ± 0.15	25.41 ± 0.51	39.91 ± 1.12
Significance	***	***	ns	*	***	ns	ns	***	**
Species × soil water content									
Bv × 80–85% FC	−1.37 ± 0.11	−1.75 ± 0.13	13.55 ± 1.78	0.24 ± 0.04	262.7 ± 11.30	4.35 ± 0.64	−0.38 ± 0.33	20.30 ± 0.93	48.92 ± 2.82
Bv × 20–25% FC	−2.35 ± 0.15	−2.35 ± 0.07	11.17 ± 1.51	0.13 ± 0.02	215.8 ± 8.77	3.08 ± 0.45	0.28 ± 0.23	25.45 ± 0.60	40.31 ± 1.60
Lp × 80–85% FC	−1.29 ± 0.03	−1.58 ± 0.07	10.07 ± 0.34	0.18 ± 0.01	280.6 ± 5.56	3.69 ± 0.24	−0.04 ± 0.13	21.06 ± 0.28	46.17 ± 0.95
Lp × 20–25% FC	−2.23 ± 0.19	−2.18 ± 0.06	9.81 ± 0.75	0.11 ± 0.02	213.9 ± 14.7	2.73 ± 0.37	0.47 ± 0.20	25.38 ± 0.91	39.51 ± 1.74
Significance	ns	ns	ns	ns	ns	ns	ns	ns	ns

ANOVA and LSD test; * $p \leq 0.05$; ** $p \leq 0.01$; *** $p \leq 0.001$; ns, not significant ($p > 0.05$); and FC, field capacity. Photo, photosynthetic rate; Cond, water conductance; Ci, intercellular CO_2 concentration; Trmmol, transpiration rate; Tl-Ta, Tleaf (temperature of leaf thermocouple)-Tair (temperature in sample cell); H_2Odiff, H_2Oi (intercellular H_2O)-H_2Os (sample cell H_2O); and RHsfc, surface humidity.

Since Photo and water status in Bv and Lp did not exhibit significant interactions, the negative effects due to water restriction were consistent for both species, which suggests that the photosynthetic ability and water status Bv and Lp behaved in a similar manner, as reflected by the WP, OP, and photosynthetic parameters (Table 2).

3.2. Traits and Adjustments of Bv and Lp Pseudostems and in Lp Stems

The response of the epidermis, parenchyma cells, and vascular bundles in the pseudostems of Lp and Bv to water restriction differed in magnitude. These structures exhibited differences in their functional role; Bv presented many lignified sclerenchyma cells (red coloured features in Figure 2A–F) arranged in the outer margin of the sheath at intervals, which supported the spatial structure of Bv pseudostems. Meanwhile, in Lp, sclerenchyma cells located on the top of the vascular bundle appeared to support the pseudostem connection with the outer epidermis (Figure 2I,J). In addition, the existence of withered pseudostems seemed to enhance the protection and support functions for living pseudostems of Lp. The pseudostems of Bv were significantly ($p \leq 0.001$; Table 3) thicker than that in Lp (Figure 2C,D vs. Figure 2I,J: 170.07 µm in Bv and 79.42 µm in Lp), suggesting that the water retention ability of Bv pseudostems was greater when compared to that of Lp. Moreover, the size of the vascular bundles in Bv was significantly larger ($p \leq 0.001$), including their diameter and area, when compared to Lp (Table 3). The pseudostems of both species had gas cavities, which may reflect the increase in parenchyma cell size and decrease in number when young pseudostems were compared to senescent pseudostems (Figure 2).

Table 3. The thickness of the pseudostem, epidermis, cuticle, bundle sheath, and bundle sheath wall, the diameter of the xylem and vascular bundle, and the vascular bundle area in the pseudostems of *Bromus valdivianus* (Bv) and *Lolium perenne* (Lp) grown at 80–85% FC and 20–25% FC. (mean ± sem; $n = 5$).

	Pseudostem T	Epidermis T	Cuticle T	Vascular Bundle				
				Xylem D	Vascu D	Vascu Area	Bun sh T	Bun sh Wall
	µm					µm^2	µm	
Species								
Bv	170.07 ± 14.29	9.08 ± 0.62	1.22 ± 0.12	11.40 ± 0.83	52.17 ± 2.31	3136 ± 290	5.07 ± 0.32	1.93 ± 0.10
Lp	79.42 ± 6.08	9.47 ± 0.46	1.72 ± 0.19	6.05 ± 0.29	35.97 ± 1.30	1355 ± 102	4.87 ± 0.20	1.07 ± 0.04
Significance	***	ns	*	***	***	***	ns	***
Soil water content								
80–85% FC	155.63 ± 16.67	10.62 ± 0.43	1.78 ± 0.20	10.06 ± 0.91	48.19 ± 2.82	2723 ± 341	5.17 ± 0.25	1.36 ± 0.09
20–25% FC	93.87 ± 8.65	7.92 ± 0.38	1.15 ± 0.10	7.39 ± 0.70	39.95 ± 2.14	1767 ± 190	4.76 ± 0.25	1.64 ± 0.16
Significance	***	***	**	***	***	***	ns	**
Species × soil water content								
Bv × 80–85% FC	218.53 ± 9.20 a	10.50 ± 0.78	1.61 ± 0.12	13.16 ± 1.21	57.71 ± 2.88	3918 ± 372 a	5.61 ± 0.39	1.68 ± 0.06 b
Bv × 20–25% FC	121.61 ± 8.73 b	7.66 ± 0.65	0.83 ± 0.08	9.63 ± 0.79	46.63 ± 2.38	2354 ± 223 b	4.52 ± 0.43	2.18 ± 0.14 a
Lp × 80–85% FC	92.73 ± 8.69 c	10.75 ± 0.53	1.96 ± 0.33	6.95 ± 0.28	38.67 ± 1.89	1529 ± 157 c	4.74 ± 0.30	1.04 ± 0.06 c
Lp × 20–25% FC	66.11 ± 4.96 c	8.19 ± 0.43	1.48 ± 0.08	5.15 ± 0.26	33.28 ± 1.11	1181 ± 87 c	5.01 ± 0.26	1.10 ± 0.06 c
Significance	***	ns	ns	ns	ns	**	ns	*

ANOVA and LSD test; * $p \leq 0.05$; ** $p \leq 0.01$; *** $p \leq 0.001$; ns, not significant ($p > 0.05$); FC, field capacity; Vascu, vascular bundle; Bun sh, bundle sheath; T, thickness; and D, diameter.

Water restriction altered the pseudostem structures of both Lp and Bv. It significantly lessened Bv pseudostem thickness ($p \leq 0.001$) and vascular bundle area ($p \leq 0.01$), as indicated by the significant interaction between species and water restriction (Table 3). In both species, the cuticle covering the epidermis became thinner, decreasing from 1.61µm to 0.83 µm (48.4% reduction) in Bv and from 1.96 µm to 1.48 µm (24% reduction) in Lp (Table 3). There was no significant interaction between species and water restriction levels. In Bv, the bundle sheath cell wall (the protective tissue of vasculatures) was strengthened under water restriction, as demonstrated via the significantly increased thickness from 1.68µm to 2.18µm. In contrast, the bundle sheath cell wall of Lp was not significantly strengthened (Table 3).

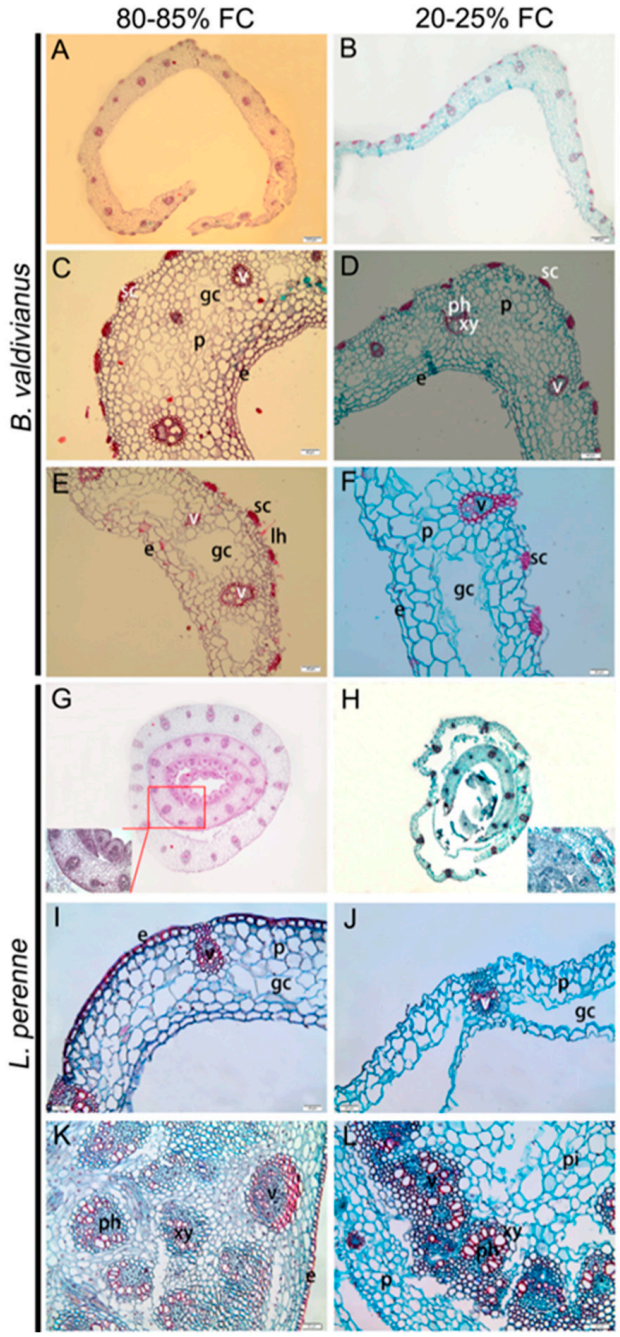

Figure 2. Anatomical pseudostem structure of *Bromus valdivianus* (Bv) and *Lolium perenne* (Lp) and stem structure of Lp exposed to two soil water restrictions. (**A**–**F**), Bv; (**G**–**L**), Lp (n = 15 per plant organ). Column 1 shows under 80~85% FC; column 2 illustrates under 20~25% FC. Rows 1~3 represent cross-sections of pseudostems of Bv; row 2 depicts a young pseudostem; row 3 illustrates a senescent pseudostem; Rows 4~5 represent Lp cross-sections of young and senescent pseudostems, respectively; row 6 depicts a stem of Lp. The images (**A**,**B**,**G**,**H**) were taken at 10 × 4; the other images were taken at 10 × 20. Scale bar = 100 µm in (**A**,**B**); 40 µm in (**C**–**E**); and 20 µm in (**F**,**I**–**L**). Letters within the images indicate: e, epidermis; gc, gas cavity; lh, leaf hair; p, parenchyma; ph, phloem; pi, pith; sc, sclerenchyma; v, vascular bundle; and xy, xylem.

At sample collection, the stem cone of Lp had grown to approximately 1.0 cm to 1.5 cm long, thus allowing stem samples to be collected. However, Bv stems were too short to be sampled. Vascular bundles of the Lp stem were developed, distributed, and varied in size. *Lolium perenne* pith cells were observed to have a nucleus inside and surrounded the vascular bundle (Figure 2K). Under water restriction, the vascular bundle arrangements of Lp changed and were dispersed around the edges of the stem (Figure 2L vs. Figure 2K) and were strengthened in the xylem vessels walls (Figure 2K vs. Figure 2L). There were no statistically significant changes in the thickness of the epidermis and cortex, diameter of the stem and vascular bundle, xylem width, and vascular bundle area in Lp stem cone due to the water restriction (Table 4).

Table 4. The thickness of the epidermis and cortex, diameter of stem, vascular bundle, and xylem, and vascular bundle area in stem in *Lolium perenne* (Lp) grown at 80–85% FC and 20–25% FC (mean ± sem; n = 5).

	Epidermis T	Stem D	Cortex T	Vascular Bundle		
				Xylem D	Vascu D	Vascu Area
			μm			μm^2
80–85% FC	7.44 ± 0.30	423.5 ± 49.5	107.22 ± 17.83	60.94 ± 3.21	6.07 ± 0.28	3777 ± 396
20–25% FC	7.25 ± 0.70	432.9 ± 24.2	63.09 ± 11.65	46.02 ± 1.75	6.80 ± 0.35	2239 ± 438
Significance	ns	ns	ns	ns	ns	ns

ANOVA and LSD test; ns, not significant ($p > 0.05$); FC, field capacity; Vascu, vascular bundle; T, thickness; and D, diameter.

3.3. Leaf Structure Traits and Leaf Adjustments to Water Restriction

Bromus valdivianus and Lp blade structures and anatomical traits are shown in Figure 3. The blade transection shapes revealed differences between both grass species in that the upper and lower epidermis were smooth and parallel in Bv (Figure 3C), while the upper surface of the Lp blade had a ribbed protuberance at the top and a few bulliform cells at the bottom of a groove. The lower surface of the Lp blade was smooth and straight (Figure 3J–M). The stomata number of Lp was lower than that of Bv (Figure 3I vs. Figure 3B), and each was located at the side of a ridge-like feature with a large gas cavity below (Figure 3J–M).

Lolium perenne had leaf hairs that were short and thorn-like (Figure 3H). *Bromus valdivianus* had many stomata arranged in rows in both the upper and lower epidermis with small gas cavities underneath (Figure 3B,C). Leaf hairs of Bv appeared to be long and dense (Figure 3A).

Bromus valdivianus and Lp responses to water restriction were verified via the thicknesses of the leaf, mesophyll, and upper epidermis (Table 5). There was no significant interaction uncovered between species and water restriction for leaf and mesophyll thickness, both at peak position. Both attributes significantly decreased their thickness at peak position due to water restriction, with leaf thickness declining from 124.38 μm to 107.62 μm ($p \leq 0.01$) and mesophyll thickness decreasing from 98.11 μm to 87.76 μm ($p \leq 0.05$) (Table 5). However, at valley position, the leaf and mesophyll thickness exhibited a significant interaction between species and water restriction in that Bv leaf valley thickness decreased from 87.68 μm to 78.73 μm ($p \leq 0.01$) and Bv mesophyll valley thickness diminished from 64.02 μm to 57.31 μm ($p \leq 0.05$), but in Lp both attributes remained unchanged as soil water restriction increased. Despite the decrease in the thickness of Bv leaf valley and mesophyll valley, both attributes continued being greater in Bv when compared to Lp (Table 5).

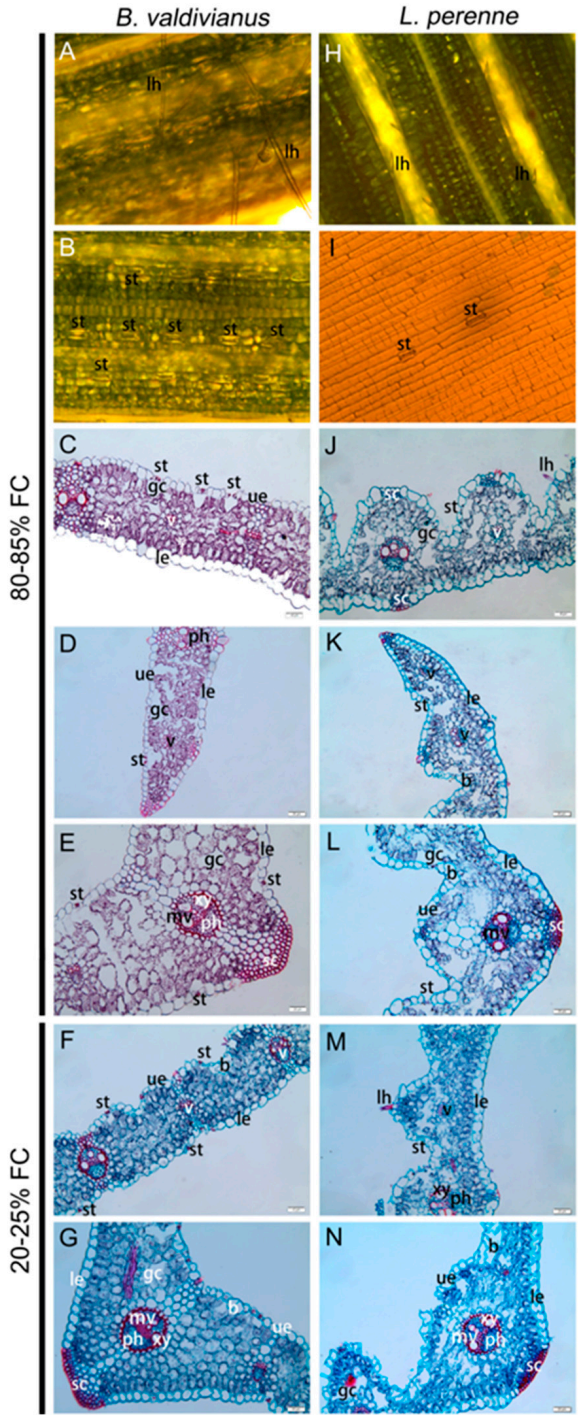

Figure 3. Blade anatomical structures of *B. valdivianus* (Bv) and *L. perenne* (Lp) exposed to 80~85% FC (**A**–**E**,**H**–**L**) and to 20~25% FC (**F**,**G**,**M**,**N**). Left column, Bv; right column, Lp. Row 1 represents a blade surface showing leaf hair. Row 2 depicts stomata in the lower surface of a blade. Rows 3 and 6 represent the cross-section of a blade. Row 4 depicts the edge of a blade. Rows 5 and Row 7 illustrate the mid-vein of a blade (n = 15 per plant organ). The images in (**A**,**B**,**H**,**I**) were taken at 6.8 times under a stereoscope; the other images were taken at 10 × 20. Scale bar = 20 μm in (**C**–**G**,**J**–**H**). Letters within the images indicate: b, bulliform; le, lower epidermis; gc, gas cavity; lh, leaf hair; mv, mid-vein; ph, phloem; sc, sclerenchyma; st stoma; ue, upper epidermis; v, vein; and xy, xylem.

The soil water restriction stimulated adjustments of the epidermis and cuticle in both species. The upper epidermis thickness was significantly reduced ($p \leq 0.05$) for both species; however, the lower epidermis thickness remained unchanged (Table 5). The upper

cuticle ($p \leq 0.01$) and lower cuticle ($p \leq 0.01$) were significantly thickened (57.3% and 38.1%, respectively) in Bv, while the upper and lower Lp cuticles did not show significant adjustments (Table 5).

There was a significant interaction between the species and the water restriction for the bulliform cell depth ($p \leq 0.001$) and mid-vein width ($p \leq 0.001$). At FC, both attributes were greater for Bv than Lp, but with water restriction, Bv bulliform cell depth significantly decreased by 20.7%, while increasing by 33.3% for Lp. The mid-vein diameter was significantly ($p \leq 0.001$) reduced by 39.5% and 21.8% for Bv (Figure 3E,G) and Lp (Figure 3L,N), respectively, both ending with similar dimensions (Table 5).

Parallel veins of both Bv and Lp differed in size and were classified as either big or small veins for interpretation of their functions (Figure 3C,D,F,J,M). *Bromus valdivianus* big veins exhibited a greater diameter ($p \leq 0.05$) and area ($p \leq 0.05$; Table 6) when compared to Lp big veins. Big veins' xylem diameter ($p \leq 0.05$) and phloem thickness ($p \leq 0.001$) were larger in Bv when compared to those in Lp. Small veins' diameter of Bv and Lp was only statistically decreased for Lp under water restriction ($p \leq 0.001$; Table 6). However, Bv small veins' area was greater than that of Lp in the control treatment ($p \leq 0.01$). Increased water restriction did not affect the small veins' area of Bv, but the small veins' area of Lp increased and was similar to that of Bv at 80–85% FC.

The diameter of both type of veins in the xylem decreased due to water restriction, equivalating to 30.8% and 24.5% for the big veins and small veins, respectively. The large and small veins in the phloem of both species did not change as a consequence of the water restriction (Table 6).

3.4. Canonical Variate Analysis of the Pseudostem and Leaf Structure

The interaction between species and water restriction was analysed via CVA, which explained 97.6% of the total differences between the treatments measured with the variables of the pseudostem structures. Wilk's Lambda was extremely significant ($p \leq 0.0001$; Figure 4). CAN 1 explained 73.9% of the differences between the treatments, which were mainly based on species differences due to morphological attributes in that Bv had a higher sheath thickness, vein area, vein diameter, and xylem values, while Lp was strongly correlated to the increase in cuticle thickness.

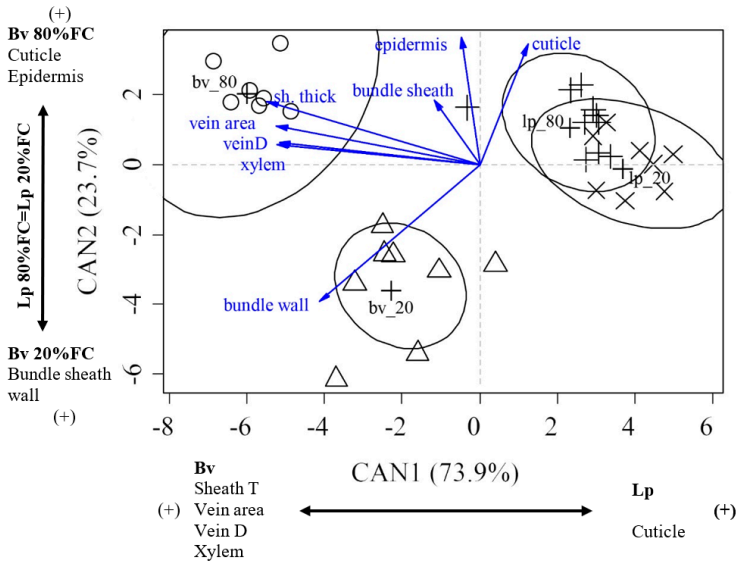

Figure 4. Canonical variate analysis (CVA) for pseudostem anatomical structures of *Bromus valdivianus* (Bv) and *Lolium perenne* (Lp) grown at 80~85% FC and 20~25% FC. CAN 1 and CAN 2 explained 97.6% of the variation among the variables and the species–water restriction interaction. Vectors indicated variables of anatomical structure. Ovals highlighted the 95% confidence interval around the means for the interaction between species and water restriction.

Table 5. The thickness of the leaf, mesophyll, epidermis, and cuticle, mid-vein diameter, and bulliform cell depth in leaf blades of *Bromus valdivianus* (Bv) and *Lolium perenne* (Lp) grown at 80–85% FC and 20–25% FC. (mean ± sem; n = 5) Unit: μm.

	Leaf T		**Mesophyll T**		**Epidermis T**		**Cuticle T**		**Mid-Vein**	**Bulliform**
	Peak	**Valley**	**Peak**	**Valley**	**Upper**	**Lower**	**Upper**	**Lower**		
Species										
Bv	105.28 ± 3.40	105.28 ± 3.40	85.37 ± 2.57	85.44 ± 2.50	10.75 ± 0.33	11.83 ± 0.48	0.88 ± 0.06	1.25 ± 0.06	215.91 ± 13.06	18.69 ± 0.66
Lp	126.72 ± 4.69	61.13 ± 2.35	100.50 ± 4.19	35.90 ± 1.37	9.90 ± 0.30	12.12 ± 0.53	0.81 ± 0.04	1.41 ± 0.05	180.19 ± 7.86	15.91 ± 0.98
Significance	***	***	**	***	ns	ns	ns	*	***	**
Soil water content										
80–85% FC	124.38 ± 4.72	87.68 ± 7.31	98.11 ± 3.85	64.02 ± 6.83	10.86 ± 0.38	12.38 ± 0.68	0.73 ± 0.04	1.25 ± 0.08	235.72 ± 12.78	17.24 ± 1.18
20–25% FC	107.62 ± 3.53	78.73 ± 3.83	87.76 ± 2.43	57.31 ± 4.53	9.79 ± 0.25	11.57 ± 0.28	0.96 ± 0.06	1.42 ± 0.04	160.38 ± 5.96	17.35 ± 0.61
Significance	**	*	*	*	*	ns	***	*	***	ns
Species × soil water content										
Bv × 80–85% FC	115.64 ± 5.16	115.6 ± 5.16 a	92.55 ± 4.40	92.69 ± 4.04 a	11.51 ± 0.48	12.81 ± 0.90	0.68 ± 0.06 b	1.05 ± 0.06 b	269.1 ± 12.46 a	20.85 ± 0.50 a
Bv × 20–25% FC	94.93 ± 2.58	94.93 ± 2.58 b	78.19 ± 1.51	78.19 ± 1.51 b	9.99 ± 0.33	10.85 ± 0.18	1.07 ± 0.07 a	1.45 ± 0.06 a	162.7 ± 7.98 c	16.53 ± 0.58 c
Lp × 80–85% FC	133.13 ± 8.09	59.73 ± 4.70 c	103.68 ± 6.82	35.35 ± 2.40 c	10.21 ± 0.49	11.94 ± 1.03	0.78 ± 0.04 b	1.44 ± 0.10 a	202.3 ± 4.57 b	13.64 ± 1.44 c
Lp × 20–25% FC	120.31 ± 4.73	62.54 ± 1.91 c	97.33 ± 3.54	36.44 ± 1.26 c	9.59 ± 0.38	12.30 ± 0.56	0.84 ± 0.07 b	1.38 ± 0.06 a	158.1 ± 3.58 c	18.18 ± 0.99 b
Significance	ns	**	ns	*	ns	ns	**	**	***	***

ANOVA and LSD test; * $p \leq 0.05$; ** $p \leq 0.01$; *** $p \leq 0.001$; ns, not significant ($p > 0.05$); FC, field capacity; and T, thickness.

Table 6. The vein diameter, xylem diameter, phloem thickness, and vein area with different sizes of blade veins of *Bromus valdivianus* (Bv) and *Lolium perenne* (Lp) grown at 80–85% FC and 20–25% FC. (mean ± sem; n = 5).

	Vein D		**Vein Area**		**Xylem D**		**Phloem T**	
	Big	**Small**	**Big**	**Small**	**Big**	**Small**	**Big**	**Small**
	μm		**μm²**		**μm**			
Species								
Bv	45.14 ± 1.59	18.89 ± 0.21	1975 ± 113	435 ± 18	11.18 ± 0.59	2.80 ± 0.15	16.95 ± 0.45	10.54 ± 0.42
Lp	39.36 ± 2.12	17.88 ± 0.69	1307 ± 83	389 ± 26	9.67 ± 0.61	2.71 ± 0.16	12.77 ± 0.60	9.75 ± 0.42
Significance	*	*	***	**	*	ns	***	ns
Soil water content								
80–85% FC	45.55 ± 1.96	19.52 ± 0.30	1822 ± 134	395 ± 26	12.32 ± 0.58	3.14 ± 0.12	15.18 ± 0.89	10.33 ± 0.40
20–25% FC	38.95 ± 1.75	17.25 ± 0.49	1460 ± 118	427 ± 19	8.53 ± 0.38	2.37 ± 0.09	14.54 ± 0.72	9.97 ± 0.47
Significance	*	***	*	*	***	***	ns	ns
Species × soil water content								
Bv × 80–85% FC	46.70 ± 2.75	19.16 ± 0.30 a	2197 ± 145	401 ± 66 a	13.17 ± 0.76	3.21 ± 0.10	17.41 ± 0.85	10.17 ± 0.66
Bv × 20–25% FC	43.59 ± 1.90	18.63 ± 0.28 a	1753 ± 145	409 ± 93 a	9.18 ± 0.48	2.38 ± 0.16	17.69 ± 0.29	10.92 ± 0.52
Lp × 80–85% FC	44.40 ± 2.42	19.88 ± 0.47 a	1447 ± 108	276 ± 55 b	11.47 ± 0.63	3.06 ± 0.21	12.95 ± 0.68	10.48 ± 0.51
Lp × 20–25% FC	34.32 ± 2.11	15.87 ± 0.23 b	1167 ± 107	387 ± 83 a	7.78 ± 0.54	2.37 ± 0.07	12.60 ± 1.01	9.02 ± 0.53
Significance	ns	***	ns	**	ns	ns	ns	ns

ANOVA and LSD test; * $p \leq 0.05$; ** $p \leq 0.01$; *** $p \leq 0.001$; ns, not significant ($p > 0.05$); FC, field capacity; T, thickness; and D, diameter.

The species responses to the water treatments were mainly described through CAN 2, which explained 23.7% of the total differences between the treatments. CAN 2 showed that increasing water restriction diminished the cuticle and epidermis width, whereas the bundle sheath wall thickness increased (Figure 4). *Lolium perenne* pseudostem structures did not present significant adjustments due to the water restriction.

The canonical variate analysis of leaf anatomical traits explained 98.1% of the total differences between treatments (Figure 5). Wilk's Lambda was extremely significant ($p \leq 0.0001$). CAN1 explained 89.4% of the differences among treatments based on species anatomical attributes, while CAN2 explained 8.7% of the differences among treatments and relied on species attribute modifications due to water restriction levels.

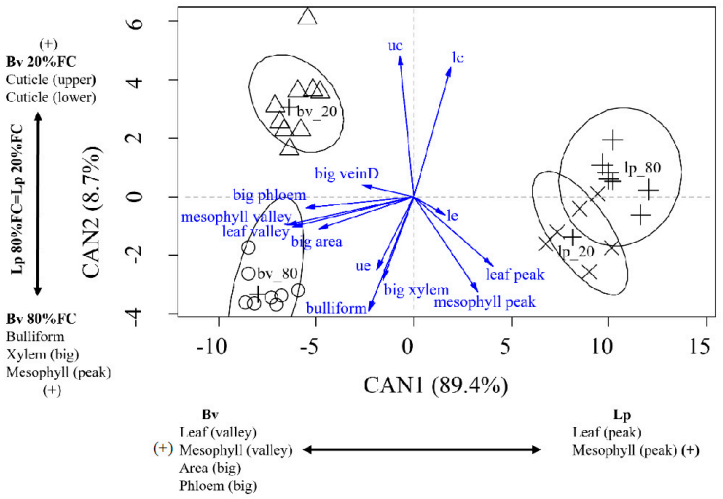

Figure 5. Canonical variate analysis for leaf blade anatomical structures of *Bromus valdivianus* (Bv) and *Lolium perenne* (Lp) grown at 80~85% FC and 20~25% FC. CAN 1 and CAN 2 explained 98.1% of the variation among the variables and the species–water restriction interaction. Vectors indicated variables of anatomical structure. Ovals highlighted the 95% confidence interval around the means for the interaction between species and water restriction.

Leaf blade anatomical trait differences between the species were shown via CAN 1 in that Bv had a larger leaf thickness (valley), mesophyll thickness (valley), wider mid-vein, and bigger phloem, while Lp had a larger leaf thickness (peak) and mesophyll thickness (peak). CAN 2 showed a contrast between the increase in the bulliform size, xylem width, and thicker mesophyll (peak), which had a strong positive relationship with Bv 80–85% FC. However, an increase in the upper and lower cuticle thickness levels of Bv was associated with increased water restriction, suggesting that the response of Bv to the water restriction was through the reduction in the bulliform size, xylem width, and mesophyll thickness (peak) (Figure 5). In addition, Lp did not exhibit significant alterations to blade structures with increasing water restriction.

4. Discussion

Plants' anatomical responses to short-term soil water restriction or long-term drought events are related to adaptive strategies expressed via resistance mechanisms [35]. The authors of [36] proposed a unified conceptual framework of plant adaptive strategies to drought, which included dehydration escape, avoidance, tolerance, dormancy, cavitation tolerance, and desiccation tolerance. These strategies can be expressed as either "drought resistance" with maintenance of aerial growth or "drought survival" after growth cessation [36].

The current study showed that soil water restriction, 20–25% of FC, triggered different short-term response mechanisms in both Lp and Bv, where growth was reduced in the short term for longer-term survival in that both species displayed drought resistance strategies that allowed plants to tolerate low tissue levels of dehydration (>30% water), as described by the authors of [36].

The analysis of photosynthetic parameters showed that the Photo of both species decreased slightly under applied soil water restriction, which was equivalent to severe drought stress (Table 2). Intercellular CO_2 concentration decreased significantly, causing stomatal limit value (Ls) increase (Ls = (1 − Ci/C0) × 100%, where C0 denotes CO_2 concentration in the air). The authors of [37] reported that Photo and Ci changes express a similar response (same direction) and Ls increases. Therefore, the decrease in photosynthesis is mainly caused by stomatal factors, rather than the decrease in mesophyll cell assimilation ability [37]. The results of our study indicated that plant water status and the structure related to stomatal function in Lp and Bv were of great significance to drought physiology response mechanisms, thereby allowing both species to tolerate the imposed soil water restriction.

4.1. Morpho-Anatomical Traits and Adjustments of Pseudostem (or Stem) Attributes Relevant to Water Movement

In the root neck, pseudostems and stems (wrapped in pseudostems) were present in Lp, whereas only pseudostems were found in Bv. The Lp vascular bundles, including the xylem and phloem, were numerous, distributed throughout the whole stem, and varied in size from small to large (Figure 2K). When Lp plants experienced water restriction, there were no significant changes ($p > 0.05$) in the stem attributes, such as the stem diameter, xylem diameter, and the diameter and area of the vascular bundle (Table 4). However, the observation and comparison of repeated stem images indicated that the xylem vessel walls became thickened and lignified (Figure 2L vs. Figure 2K). These adjustments of the vessel walls strengthen longitudinal water movement [38], which support apical meristem growth. These Lp stem anatomical traits explain, in part, the high increase in Lp tiller number under either irrigation or soil water restriction [39] when compared to Bv (Figure 1 and Table 1).

The Lp pseudostem anatomical structure was not largely modified under water stress. The thick cuticle covering on the epidermis cells probably contributed to the avoidance of water loss during water restriction.

Bromus valdivianus generated a more developed pseudostem than Lp (Table 2; Figure 2C,D vs. Figure 2I,J). Thicker pseudostems ($p \leq 0.001$) with bigger diameter vascular bundles (including bigger xylem) with a larger area ($p \leq 0.001$; Table 3) result in the xylem becoming a low-resistance pathway for water flow in vascular plants [38,40]. In addition, Bv pseudostems are largely composed of parenchyma cells. Parenchyma cells can form various organs in plants due to their high plasticity and totipotency [38], for example, pith parenchyma, cortical parenchyma, leaf mesophyll, and epidermis. Thus, it has multiple functions, such as photosynthesis (chloroenchyma) [41], protection and storage (epidermis and cortex) [15], wound repair [42], and conduction (xylem and phloem) [40]. According to previous research, pseudostem parenchyma cells may be associated with plant water status through plant water conduction and water storage. In the current study, Bv pseudostem parenchyma cells were ~20 layers thick (Figure 2C), which would allow for the storage of a large amount of water to support canopy growth. This suggests a structural foundation explaining Bv as a six-leaf grass species [25]. In contrast to Bv, Lp pseudostems presented <10 layers of parenchyma cells (Figure 2I), which may explain Lp as a three-leaf species [43].

We observed a significant ($p \leq 0.05$) adjustment of the Bv pseudostem in response to soil water restriction in that the bundle sheath cell wall thickened from 1.68 µm to 2.18 µm (Table 3; Figure 5). Heinen et al. [44] described bundle sheath cells controlling and regulating water transport between membranes through aquaporins. Shatil-Cohen [45] reported that bundle sheath cell regulation of xylem–mesophyll water transport plays an important role in maintaining leaf water potential in *Arabidopsis thaliana* (L.) Heynh under water stress. In the present study, the thickness of the Bv bundle sheath wall also enhanced drought tolerance (Figure 5). We suggest that one function of the bundle sheath cell wall was to prevent water diffusion from the vascular bundle to the pseudostem, thereby minimising water-conducting loss; however, this interpretation needs to be verified.

Moreover, as a response to soil water restriction, vascular bundle area decreased in Bv, which would confer a greater surface-to-volume ratio to maintain the water column continuity in higher tensions, thereby preventing embolism [7,46]. This attribute has been described as a plastic response of grasses to soil water restrictions [46].

4.2. Morpho-Anatomical Traits and Adjustments of Leaf Blade Structures Relevant to Water Evaporation and Transpiration

Leaves are directly exposed to the air and constitute the plant organ that regulates gas exchange (water vapor and CO_2) between the plant–air complex. Most plant water loss occurs through leaf transpiration with or without passing through stomatal pores [47]. Trlica and Biondini [48] reported that water loss through transpiration significantly decreases as leaf area decreases, as described for *Pascopyrum smithii* (Rydb.) A. Love (western wheatgrass) in relation to *Bouteloua gracilis* (Willd. Ex Kunth) Lag. Ex Griffiths (blue grama) and *Agropyron cristatum* (L.) Gaertn. (crested wheatgrass). In the present study, Lp upper blade surface had a ribbed protuberance or corrugated-like shape (Figure 3J–M), as described by the authors of [43,49]. This trait may reflect a large percentage of direct light under high light conditions contributing to lower heat absorption and transpiration, and aid in diffused light capture for photosynthesis, for example, from multiple directions in cloudy conditions [50,51]. Stomata control water and gas exchange, directly regulating plant transpiration [52,53]. We observed that Lp stomata were located at the side of a ribbed protuberance in the upper blade surface (Figure 3J–M). We suggested that the narrow outer space formed via the ribbing/corrugation would help to trap cooler moist air and maintain the relative humidity of the leaf surface.

Plant strategies to withstand limited water availability frequently rely on morphological traits that confer water preservation capacity to stressed tissues, such as greater leaf thickness, low leaf area-to-volume ratio, high trichome (leaf hair) density, and thick leaf cuticle [54,55]. Therefore, leaf traits are important and relevant as criteria to select drought-tolerant phenotypes. The present study found that Lp has a greater leaf thickness and mesophyll thickness at peak position, structures that are beneficial to plant water storage, as well as lower water potential and osmotic potential under water restriction. The significant diminishment of the WP and OP exhibited by Lp and Bv correspond to a strategy that enhances water acquisition and water conservation abilities with increasing soil water restriction [56].

In addition, the depth of the bulliform cells, thin-walled water-containing cells, greatly increased in Lp leaf blades under water restriction when compared with the control ($p \leq 0.001$; Table 4). This facilitates rolling of the leaf blade to avoid water loss during water stress [57–59] in that when the soil water supply is restricted, the bulliform cells first lose water and then shrink; this curls the leaves into a tubular shape, decreasing the leaf blade's evaporation area and water loss [60]. When water is available, the bulliform cells fill and flatten/uncurl the leaves [61].

Leaf hairs constitute a physical barrier on plant surfaces against biotic [62] and abiotic stresses [63,64], including drought [65], pathogens [62], and UV light [66]. Hairy leaves of *Mallotus macrostachyus* (Miq.) Müll. Arg. contribute to a high water-use efficiency (WUE) and to a low transpiration rate during drought conditions, when compared with denuded leaves [67]. Leaf hairs increased their resistance to water loss, leading to reduced transpiration and higher leaf WUE [66]. In many xerophytic plants, long leaf hairs are an effective adaptation to low rainfall environments [68], and the number of leaf hairs has been used as a morphological indicator for drought and insect resistance [63]. *Bromus valdivianus* has long and dense leaf hairs and indicates a certain tolerance to soil water restriction (Figure 3A). *Lolium perenne* was observed to have leaf hairs that were short and thorn-like (Figure 3H).

The stomata in Lp were less numerous and distributed at the side of a ridge with a large gas cavity under each stoma (Figure 3J–M) when compared to Bv (Figure 3I vs. Figure 3B). *Bromus valdivianus* had many stomata arranged in rows in both the upper

and lower epidermis with a small gas cavity under each (Figure 3B,C). Plant soil water restriction/stress was intimately linked with plant stomata size, density, and water-use efficiency. There is a negative relationship between stomata density and stomata size [69,70] in that small and abundant stomata imply a faster response to prevent water loss, enhancing fine regulation of plant water utilisation by improving short-term water use [71]. Increasing stomata density and size diminishment constitutes an ecological indicator (genetic factor) for the degree of plant water stress tolerance, which has been linked to species from xeric environments [70,72,73], and has been utilised in the selection and improvement of plant WUE [73]. In addition, stomata size and density are inversely related and constitute a phenotypic plasticity response that contributes to short-term water use regulation [73,74].

The cuticle is a thin continuous layer that covers the surface of all epidermal cell types and acts as a hydrophobic barrier [75,76] due to the presence of insoluble polymeric cutin and soluble waxes [8]. It protects plants from adverse environmental conditions and contributes to water conservation [77,78]. In the current study, the cuticles of Bv had a significant increase in their thickness in the upper and lower epidermis when it was subjected to water restriction (Table 5). The canonical variate analysis also indicated that increasing cuticle thickness in both sides of the Bv leaf blade was a positive response to soil water restriction (Figure 5), which limited plant water loss. Research has demonstrated an inverse relationship between cuticle thickness and epidermal water loss in *Zea mays* L. [8], *Sorghum bicolor* (L.) Moench [79], and *Suaeda maritima* (L.) Dum. [80], suggesting that a thick cuticle covering on the epidermis reduces water loss via non-stomatal transpiration.

Bromus valdivianus pseudostem and blade attributes, including dense hairs, stomata number and cuticle, and epidermis thickness, are structures that are directly and indirectly integrated into a drought response, which regulates plant water loss and movement. Active integration of these mechanisms contributes to the Bv drought-tolerant mechanism, as reported by the authors of [18,31], thereby providing stability to pasture systems from the spring through the dry summer season into autumn [81]. This current study provides clear, quantifiable results elucidating the structural and physiological mechanisms triggered in Lp and Bv via severe water restriction. This study also highlights the ongoing challenges faced by pasture production systems in response to global climate change drivers, and explains, in part, why both Lp and Bv persist and co-dominate in productive temperate humid climate pasture systems [20].

5. Conclusions

Severe soil water restriction greatly reduced the growth, photosynthesis, and water status of Bv and Lp. Attributes that supported Lp growth during water restriction included well-developed vascular bundles in the stem, along with the following anatomical leaf traits: corrugated shape of its upper surface, stomata spatial location, and thick leaf and mesophyll at peak position. Functional mechanisms of Lp under water restriction included thickened and lignified xylem vessel walls in the stem to ensure water movement inside the plant, and deepened bulliform cells in the leaves to enhance leaf curling, which contributes to reduced water loss.

Bromus valdivianus is a water restriction-tolerant species when its attributes are combined. The attributes included the many layers of parenchyma cells in the pseudostems, long and dense leaf hairs, and small, numerous stomata in the leaves. The response of *Bromus valdivianus* to the water restriction was verified via increased thickness of the pseudostem bundle sheath wall and the upper and lower epidermis cuticle, which favoured water flow and water loss reduction.

Although both grass species were adapted to drought conditions, they differed in their morpho-anatomical mechanisms to reach similar physiological functions to reduce water loss. These attributes explain how these pasture species have enhanced persistence and resilience under soil water restriction.

Author Contributions: Y.Z., J.G.-F., I.F.L., I.P.O., A.D.C. and P.D.K., writing original draft preparation; Y.Z., J.G.-F., H.H., I.F.L. and I.P.O., methodology; I.F.L. and J.G.-F., statistics software and data analysis; I.F.L. and A.D.C., funding acquisition. All authors have read and agreed to the published version of the manuscript.

Funding: This research received no external funding.

Data Availability Statement: Data is available upon request from corresponding author.

Acknowledgments: We gratefully thank Xiongzhao He for his support in photomicrography, Xialin Zheng and Ying Wang for providing help in processing and analysing images, as well as to Lesly Taylor, Zhuo Yang, and Lulu He for their help and support at the Plant Growth Unit, Massey University. We thank Massey University Research Fund (MURF) and the T. R. Ellett Agricultural Research Trust for financial support.

Conflicts of Interest: The authors declare no conflict of interest.

References

1. Seneviratne, S.I.; Zhang, X.; Adnan, M.; Badi, W.; Dereczynski, C.; Di Luca, A.; Ghosh, S.; Iskandar, I.; Kossin, J.; Lewis, S.; et al. Weather and Climate Extreme Events in a Changing Climate. In *Climate Change 2021: The Physical Science Basis. Contribution of Working Group I to the Sixth Assessment Report of the Intergovernmental Panel on Climate Change*; Masson-Delmotte, V., Zhai, P., Pirani, A., Connors, S.L., Péan, C., Berger, S., Caud, N., Chen, Y., Goldfarb, L., Gomis, M.I., et al., Eds.; Cambridge University Press: Cambridge, UK, 2021; pp. 1513–1766. [CrossRef]
2. Vicente-Serrano, S.M.; Peña-Angulo, D.; Beguería, S.; Domínguez-Castro, F.; Tomás-Burguera, M.; Noguera, I.; Gimeno-Sotelo, L.; El Kenawy, A. Global drought trends and future projections. *Philos. Trans. R. Soc. A* **2022**, *380*, 20210285. [CrossRef] [PubMed]
3. Malinowski, D.P.; Kigel, J.; Pinchak, W.E. Water deficit, heat tolerance, and persistence of summer-dormant grasses in the U.S. southern plains. *Crop Sci.* **2009**, *49*, 2363–2370. [CrossRef]
4. Lens, F.; Picon-Cochard, C.; Delmas, C.E.L.; Signarbieux, C.; Buttler, A.; Cochard, H.; Jansen, S.; Chauvin, T.; Doria, L.C.; Arco, M.D.; et al. Herbaceous angiosperms are not more vulnerable to drought-induced embolism than angiosperm trees. *Plant Physiol.* **2016**, *172*, 661–667. [CrossRef] [PubMed]
5. Jacob, V.; Choat, B.; Churchill, A.C.; Zhang, H.; Barton, V.M.; Krishnananthaselvan, A.; Post, A.K.; Power, S.A.; Medlyn, B.; Tissue, D.T. High safety margins to drought-induced hydraulic failure found in five pasture grasses. *Plant Cell Environ.* **2022**, *45*, 1631–1646. [CrossRef] [PubMed]
6. Assuero, S.G.; Matthew, C.; Kemp, P.D.; Latch, G.C.M.; Barker, D.J.; Haslett, S.J. Morphological and physiological effects of water deficit and endophyte infection on contrasting tall fescue cultivars. *N. Z. J. Agric. Res.* **2000**, *43*, 49–61. [CrossRef]
7. Volaire, F.; Lens, F.; Cochard, H.; Xu, H.; Chacon-Doria, L.; Bristiel, P.; Balachowski, J.; Rowe, N.; Violle, C.; Picon-Cochard, C. Embolism and mechanical resistances play a key role in dehydration tolerance of a perennial grass *Dactylis glomerata* L. *Ann. Bot.* **2018**, *122*, 325–336. [CrossRef]
8. Ristic, Z.; Jenks, M.A. Leaf cuticle and water loss in maize lines differing in dehydration avoidance. *J. Plant Physiol.* **2002**, *159*, 645–651. [CrossRef]
9. Pitman, W.D.; Holte, C.; Conrad, B.E.; Bashaw, E.C. Histological differences in moisture stressed and non-stressed kleingrass forage. *Crop Sci.* **1983**, *23*, 793–795. [CrossRef]
10. Sultan, S.E. Evolutionary implications of phenotypic plasticity in plants. *Evol. Biol.* **1987**, *21*, 127–178.
11. Begon, M.; Harper, J.L.; Townsend, C.R. *Ecology: Individuals, Populations and Communities*; Blackwell Science: Oxford, UK, 1996.
12. López, I.F.; Balocchi, O.A.; Kemp, P.D.; Valdés, C. Phenotypic variability in *Holcus lanatus* L. in Southern Chile: A strategy that enhances plant survival and pasture stability. *Crop Pasture Sci.* **2009**, *60*, 768–777. [CrossRef]
13. Makbul, S.; Coşkunçelebi, K.; Türkmen, Z.; Beyazoglu, O. Morphology and anatomy of *Scrophularia* L. (Scrophulariaceae) taxa from NE Anatolia. *Acta Biol. Cracoviensia Ser. Bot.* **2006**, *48*, 33–43. [CrossRef]
14. Makbul, S.; Türkmen, Z.; Coşkunçelebi, K.; Beyazoglu, O. Anatomical and pollen characters in the genus *Epilobium* L. (Onagraceae) from northeast Anatolia. *Acta Biol. Cracoviensia Ser. Bot.* **2008**, *50*, 51–62.
15. Oliveira, I.; Meyer, A.; Afonso, S.; Gonalves, B. Compared leaf anatomy and water relations of commercial and traditional *Prunus dulcis* (Mill.) cultivars under rain-fed conditions. *Sci. Hortic.* **2018**, *229*, 226–232. [CrossRef]
16. Brent, D.B.; David, K.; Adam, J.L.; James, B. Evaluation of turf-type interspecific hybrids of meadow fescue with perennial ryegrass for improved stress tolerance. *Crop Sci.* **2014**, *54*, 355–365. [CrossRef]
17. López, I.F.; Kemp, P.D.; Dörner, J.; Descalzi, C.A.; Balocchi, O.A.; García, S. Competitive strategies and growth of neighbouring *Bromus valdivianus* Phil. And *Lolium perenne* L. plants under water restriction. *J. Agron. Crop Sci.* **2013**, *199*, 449–459. [CrossRef]
18. Ordóñez, I.; López, I.F.; Kemp, P.D.; Descalzi, C.A.; Horn, R.; Zúñiga, F.; Dorota, D.; Dörner, J. Effect of pasture improvement managements on physical properties and water content dynamics of a volcanic ash soil in southern Chile. *Soil Tillage Res.* **2018**, *178*, 55–64. [CrossRef]

19. Calvache, I.; Balocchi, O.; Alonso, M.; Keim, J.P.; López, I. Water-soluble carbohydrate recovery in pastures of perennial ryegrass (*Lolium perenne* L.) and pasture brome (*Bromus valdivianus* Phil.) under two defoliation frequencies determined by thermal time. *Agriculture* **2020**, *10*, 563–574. [CrossRef]
20. Ordóñez, I.P.; López, I.F.; Kemp, P.D.; Donaghy, D.J.; Herrmann, P.; Hernández, F.; Bhatia, S. Pasture brome (*Bromus valdivianus*) leaf growth physiology: A six leaf grass species. *Agron. N. Z.* **2017**, *47*, 13–22.
21. López, I.; Balocchi, O.; Lailhacar, P.; Oyarzún, C. Characterization of the growing sites of six native and naturalized species in the Humid Dominion of Chile. *Agro Sur* **1997**, *25*, 62–80. [CrossRef]
22. Olmos, E.; Sanchez-Blanco, M.J.; Fernandez, T.; Alarcón, J.J. Subcellular effects of drought stress in *Rosmarinus officinalis*. *Plant Biol.* **2007**, *9*, 77–84. [CrossRef]
23. Makbul, S.; Güler, N.S.; Durmus, N.; Güven, S. Changes in anatomical and physiological parameters of soybean under drought stress. *Turk. J. Bot.* **2011**, *35*, 369–377. [CrossRef]
24. Saha, P.; Sade, N.; Arzani, A.; Wilhelmi, M.M.R.; Coe, K.M.; Li, B.; Blumwald, E. Effects of abiotic stress on physiological plasticity and water use of *Setaria viridis* (L.) P. Beauv. *Plant Sci.* **2016**, *251*, 128–138. [CrossRef] [PubMed]
25. Ordóñez, I.P.; López, I.F.; Kemp, P.D.; Donaghy, D.J.; Zhang, Y.; Herrmann, P. Response of *Bromus valdivianus* (pasture brome) growth and physiology to defoliation frequency based on leaf stage development. *Agronomy* **2021**, *11*, 2058–2075. [CrossRef]
26. López, I.F.; Balocchi, O.A.; Alvarez, X.; Flores, P.; Latrille, L. Selectivity of *Bromus valdivianus* Phil., *Lolium perenne* L. and *Agrostis capillaris* L. by grazing dairy cows. *Agro Sur* **2016**, *44*, 53–65. [CrossRef]
27. Fulkerson, W.J.; Slack, K. Leaf number as a criterion for determining defoliation time for *Lolium perenne*, 1. Effect of water-soluble carbohydrates and senescence. *Grass Forage Sci.* **1994**, *49*, 373–377. [CrossRef]
28. Fulkerson, W.J.; Donaghy, D.J. Plant-soluble carbohydrate reserves and senescence—Key criteria for developing an effective grazing management system for ryegrass-based pastures: A review. *Aust. J. Exp. Agric.* **2001**, *41*, 261–275. [CrossRef]
29. García-Favre, J.; López, I.F.; Cranston, L.M.; Donaghy, D.J.; Kemp, P.D.; Ordóñez, I.P. Functional contribution of two perennial grasses to enhance pasture production and drought resistance under a leaf regrowth stage defoliation criterion. *J. Agron. Crop Sci.* **2022**, *209*, 144–160. [CrossRef]
30. Steel, R.G.D.; Torrie, J.H.; Dickey, D.A. *Principles and Procedures of Statistics: A Biometrical Approach*; McGraw-Hill: New York, NY, USA, 1997.
31. Descalzi, C.; Balocchi, O.; López, I.; Kemp, P.; Dörner, J. Different soil structure and water conditions affect the growing response of *Lolium perenne* L. and *Bromus valdivianus* Phil. Growing alone or in mixture. *J. Soil Sci. Plant Nutr.* **2018**, *18*, 617–635. [CrossRef]
32. Zhang, Y.; Ma, H.; Calderón-Urrea, A.; Tian, C.; Bai, X.; Wei, J. Anatomical changes to protect organelle integrity account for tolerance to alkali and salt stress in *Melilotus offincinalis*. *Plant Soil* **2016**, *406*, 327–340. [CrossRef]
33. Ruzin, S.E. *Plant Micro Technique and Microscopy*; Oxford University Press: Oxford, UK, 1999.
34. Elliot, J.; Marsh, C. *Exploring Data: An Introduction to Data Analysis for Social Scientists*; Polity Press: Cambridge, UK, 2008; ISBN-13: 978-0-7456-2282-8.
35. Haffani, S.; Mezni, M.; Nasri, M.B.; Chaibi, W. Comparative leaf water relations and anatomical responses of three vetch species (*Vicia narbonensis* L., *V. sativa* L. and *V. villosa* Roth.) to cope with water stress. *Crop Pasture Sci.* **2017**, *68*, 691–702. [CrossRef]
36. Volaire, F. A unified framework of plant adaptive strategies to drought: Crossing scales and disciplines. *Glob. Chang. Biol.* **2018**, *24*, 2929–2938. [CrossRef] [PubMed]
37. Farquhar, G.D.; Sharkey, T.D. Stomatal conductance and photosynthesis. *Ann. Rev. Plant Physiol.* **1982**, *33*, 317–345. [CrossRef]
38. Crang, R.; Lyons-Sobaski, S.; Wise, R. *Plant Anatomy: A Concept-Based Approach to the Structure of Seed Plants*; Springer Nature: Cham, Switzerland, 2018.
39. Yang, J.Z.; Matthew, C.; Rowland, R.E. Tiller axis observations for perennial ryegrass (*Lolium perenne*) and tall fescue (*Festuca arundinacea*): Number of active phytomers, probability of tiller appearance, and frequency of root appearance per phytomer for three cutting heights. *N. Z. J. Agric. Res.* **1998**, *41*, 11–17. [CrossRef]
40. Barceló, A.R. Xylem parenchyma cells deliver the H_2O_2 necessary for lignification in differentiating xylem vessels. *Planta* **2005**, *220*, 747–756. [CrossRef] [PubMed]
41. Seeni, S.; Mariappan, T.; Gopalan, G.; Gnanam, A. Mechanical separation of palisade and spongy-parenchyma cells from the leaves of mesomorphic dicotyledons for photosynthetic studies. *Planta* **1983**, *157*, 105–110. [CrossRef] [PubMed]
42. Vasyukova, N.I.; Chalenko, G.I.; Gerasimova, N.G.; Ozeretskovskaya, O.L. Wound repair in plant tissues (Review). *Appl. Biochem. Microbiol.* **2011**, *47*, 253–258. [CrossRef]
43. Soper, K.; Mitchell, K.J. The developmental anatomy of perennial ryegrass (*Lolium perenne* L.). *N. Z. J. Sci. Technol.* **1956**, *37*, 484–504.
44. Heinen, R.B.; Ye, Q.; Chaumont, F. Role of aquaporins in leaf physiology. *J. Exp. Bot.* **2009**, *60*, 2971–2985. [CrossRef]
45. Shatil-Cohen, A.; Attia, Z.; Moshelion, M. Bundle-sheath cell regulation of xylem-mesophyll water transport via aquaporins under drought stress: A target of xylem-borne ABA? *Plant J.* **2011**, *67*, 72–80. [CrossRef]
46. Vasellati, V.; Oesterheld, M.; Medan, D.; Loret, J. Effects of flooding and drought on the anatomy of *Paspalum dilatatum*. *Ann. Bot.* **2001**, *88*, 355–360. [CrossRef]
47. Šantruček, J. Transpiration efficiency and apparent cuticular transpiration in some C_3 and C_4 plants. *Biol. Plant.* **1991**, *33*, 192–199. [CrossRef]

48. Trlica, M.J.; Biondini, M.E. Soil water dynamics, transpiration, and water losses in a crested wheatgrass and native shortgrass ecosystem. *Plant Soil* **1990**, *126*, 187–201. [CrossRef]
49. Charles-Edwards, D.A.; Sant, C.E.I. Models for mesophyll cell arrangement in leaves of ryegrass (*Lolium perenne* L.). *Planta* **1972**, *104*, 297–305. [CrossRef]
50. Oguchi, R.; Onoda, Y.; Terashima, I.; Tholen, D. Leaf anatomy and function. In *The Leaf: A Platform for Performing Photosynthesis*; Adams, W.W., III, Terashima, I., Eds.; Springer: Cham, Switzerland, 2018; pp. 97–139. [CrossRef]
51. Nilsen, E.T.; Forseth, I.N., Jr. The role of leaf movements for optimizing photosynthesis in relation to environmental variation. In *The Leaf: A Platform for Performing Photosynthesis*; Adams, W.W., III, Terashima, I., Eds.; Springer: Cham, Switzerland, 2018; pp. 401–423. [CrossRef]
52. Li, K.; Huang, J.; Song, W.; Wang, J.; Wang, X. Automatic segmentation and measurement methods of living stomata of plants based on the CV model. *Plant Methods* **2019**, *15*, 67–78. [CrossRef] [PubMed]
53. Hetherington, A.M.; Woodward, F.I. The role of stomata in sensing and driving environmental change. *Nature* **2003**, *424*, 901–908. [CrossRef] [PubMed]
54. Lyshede, O.B. Xeromorphic features of three stem assimilants in relation to their ecology. *Bot. J. Linn. Soc.* **1979**, *78*, 85–98. [CrossRef]
55. Jäger, K.; Fábián, A.; Eitel, G.; Szabó, L.; Deák, C.; Barnabás, B.; Papp, I. A morpho-physiological approach differentiates bread wheat cultivars of contrasting tolerance under cyclic water stress. *J. Plant Physiol.* **2014**, *171*, 1256–1266. [CrossRef]
56. Hoover, D.; Koriakin, K.; Albrigtsen, J.; Ocheltree, T. Comparing water-related plant functional traits among dominant grasses of the Colorado Plateau: Implications for drought resistance. *Plant Soil* **2019**, *441*, 207–218. [CrossRef]
57. Abernethy, G.A.; Fountain, D.W.; Mcmanus, M.T. Observations on the leaf anatomy of Festuca novae-zelandiae and biochemical responses to a water deficit. *N. Z. J. Bot.* **1998**, *36*, 113–123. [CrossRef]
58. Balsamo, R.A.; Willigen, C.V.; Bauer, A.M.; Farrant, J. Drought tolerance of selected Eragrostis species correlates with leaf tensile properties. *Ann. Bot.* **2006**, *97*, 985–991. [CrossRef]
59. Alvarez, J.M.; Rocha, J.F.; Machado, S.R. Bulliform cells in *Loudetiopsis chrysothrix* (Nees) Conert and *Tristachya leiostachya* Nees (Poaceae): Structure in relation to function. *Braz. Arch. Biol. Technol.* **2008**, *51*, 113–119. [CrossRef]
60. Dickison, W.C. *Integrative Plant Anatomy*; Harcourt Academic Press: New York, NY, USA, 2000.
61. Grigore, M.N.; Toma, C. Bulliform Cells. In *Anatomical Adaptations of Halophytes*; Springer: Cham, Switzerland, 2017; pp. 325–338. [CrossRef]
62. Kim, S.H.; Park, S.H.; Woo, J.H.; Choi, S.Y. Hairs as physical barrier against adhesion of *Xanthomonas axonopodis* pv. Glycines on soybean leaf. *Res. Plant Dis.* **2015**, *21*, 40–43. [CrossRef]
63. Roy, B.A.; Stanton, M.L.; Eppley, S.M. Effects of environmental stress on leaf hair density and consequences for selection. *J. Evol. Biol.* **1999**, *12*, 1089–1103. [CrossRef]
64. Zhang, W.; Mirlohi, S.S.; Li, X.; He, Y. Identification of functional single-nucleotide polymorphisms affecting leaf hair number in *Brassica rapa*. *Plant Physiol.* **2018**, *177*, 490–503. [CrossRef] [PubMed]
65. Ehleringer, J.R.; Mooney, H.A. Leaf hairs: Effects on physiological activity and adaptive value to a desert shrub. *Oecologia* **1978**, *37*, 183–200. [CrossRef] [PubMed]
66. Ripley, B.S.; Pammenter, N.W.; Smith, V.R. Function of leaf hairs revisited: The hair layer on leaves *Arctotheca populifolia* reduces photoinhibition, but leads to higher leaf temperatures caused by lower transpiration rates. *J. Plant Physiol.* **1999**, *155*, 78–85. [CrossRef]
67. Kenzo, T.; Yoneda, R.; Azani, M.A.; Majid, N.M. Changes in leaf water use after removal of leaf lower surface hairs on *Mallotus macrostachyus* (Euphorbiaceae) in a tropical secondary forest in Malaysia. *J. For. Res.* **2008**, *13*, 137–142. [CrossRef]
68. Shields, L.M. Leaf xeromorphy as related to physiological and structural influences. *Bot. Rev.* **1950**, *16*, 399–447. [CrossRef]
69. Spence, R.D.; Wu, H.; Sharpe, P.J.H.; Clark, K.G. Water stress effects on guard cell anatomy and the mechanical advantage of the epidermal cells. *Plant Cell Environ.* **1986**, *9*, 197–202. [CrossRef]
70. Galmés, J.; Flexas, J.; Savé, R.; Medrano, H. Water relations and stomatal characteristics of Mediterranean plants with different growth forms and leaf habits: Responses to water stress and recovery. *Plant Soil* **2007**, *290*, 139–155. [CrossRef]
71. Franks, P.J.; Beerling, D.J. Maximum leaf conductance driven by CO_2 effects on stomatal size and density over geologic time. *Proc. Natl. Acad. Sci. USA* **2009**, *106*, 10343–10347. [CrossRef] [PubMed]
72. Ganeva, T.; Uzunova, K.; Koleva, D. Comparative leaf epidermis investigation in species of genus *Crataegus* L. (Rosaceae) from Bulgaria. *Feddes Repert.* **2009**, *120*, 169–184. [CrossRef]
73. Bertolino, L.T.; Caine, R.S.; Gray, J.E. Impact of stomatal density and morphology on water-use efficiency in a changing world. *Front. Plant Sci.* **2019**, *10*, 225–235. [CrossRef] [PubMed]
74. Xu, Z.; Zhou, G. Responses of leaf stomatal density to water status and its relationship with photosynthesis in a grass. *J. Exp. Bot.* **2008**, *59*, 3317–3325. [CrossRef] [PubMed]
75. Heredia, A.; Dominguez, E. The plant cuticle: A complex lipid barrier between the plant and the environment. In *Counteraction to Chemical and Biological Terrorism in East European Countries*; Dishovsky, C., Pivovarov, A., Eds.; Springer Nature: Cham, Switzerland, 2009; pp. 109–116.
76. Holloway, P.J. Structure and histochemistry of plant cuticular membranes: An overview. In *The Plant Cuticle*; Price, C.E., Ed.; Academic Press: London, UK, 1982; pp. 1–32.

77. Schweizer, P.; Felix, G.; Buchala, A.; Müller, C.; Métraux, J.P. Perception of free cutin monomers by plant cells. *Plant J.* **1996**, *10*, 331–341. [CrossRef]
78. Suh, M.C.; Samuels, A.L.; Jetter, R.; Kunst, L.; Pollard, M.K.; Pollard, M.; Ohlrogge, J.; Beisson, F. Cuticular lipid composition, surface structure, and gene expression in arabidopsis stem epidermis. *Plant Physiol.* **2005**, *139*, 1649–1665. [CrossRef] [PubMed]
79. Jenks, M.A.; Joly, R.J.; Peters, P.J.; Rich, P.J.; Axtell, J.D.; Ashworth, E.N. Chemically induced cuticle mutation affecting epidermal conductance to water vapor and disease susceptibility in *Sorghum bicolor* (L.) Moench. *Plant Physiol.* **1994**, *105*, 1239–1245. [CrossRef]
80. Hajibagheri, M.A.; Hall, J.L.; Flowers, T.J. The structure of the cuticle in relation to cuticular transpiration in leaves of the halophyte *Suaeda maritima* (L.) Dum. *New Phytol.* **1983**, *94*, 125–131. [CrossRef]
81. Descalzi, C.A.; López, I.F.; Kemp, P.D.; Dörner, J.; Ordóñez, I. Pasture restoration improvement methods for temperate degraded pastures and consequences of the climatic seasonality on soil–pasture complex. *J. Agron. Crop Sci.* **2020**, *206*, 130–147. [CrossRef]